# Spin Pumping by Parametrically Excited Exchange Magnons

C. W. Sandweg,[1,*] Y. Kajiwara,[2] A. V. Chumak,[1] A. A. Serga,[1] V. I. Vasyuchka,[1] M. B. Jungfleisch,[1] E. Saitoh,[2,3,4] and B. Hillebrands[1]

[1]*Fachbereich Physik and Forschungszentrum OPTIMAS, Technische Universität Kaiserslautern, 67663 Kaiserslautern, Germany*
[2]*Institute for Materials Research, Tohoku University, Sendai 980-8577, Japan*
[3]*CREST, Japan Science and Technology Agency, Sanbancho, Tokyo 102-0075, Japan*
[4]*Advanced Science Research Center, Japan Atomic Energy Agency, Tokai 319-1195, Japan*

(Received 11 March 2011; published 23 May 2011)

We experimentally show that exchange magnons can be detected by using a combination of spin pumping and the inverse spin-Hall effect proving its wavelength integrating capability down to the submicrometer scale. The magnons were injected in a ferrite yttrium iron garnet film by parametric pumping and the inverse spin-Hall effect voltage was detected in an attached Pt layer. The role of the density, wavelength, and spatial localization of the magnons for the spin pumping efficiency is revealed.

DOI: 10.1103/PhysRevLett.106.216601 PACS numbers: 72.25.Pn, 75.30.Ds, 75.76.+j, 85.75.−d

Spintronics, the field of spin-based data storage and processing, is a very promising candidate to overcome the limits of conventional charge-based electronics [1]. The spin pumping effect turned out to be an important mechanism for the generation of a spin current in nonmagnetic conductors [2,3]. The inverse spin-Hall effect (ISHE) can subsequently be used to convert this spin current into a detectable charge current [4]. It has been shown recently that it is even possible to develop magnetic insulator based spintronic devices in which the information is carried by magnons, the quanta of spin waves, instead of spin-polarized electrons [5,6].

Two different ways are often used to excite magnons. The first one is force excitation using a microwave magnetic field with the same frequency as the spin wave. With this method the wavelength of the excited spin waves is restricted by the lateral size of the antenna and mostly dipolar magnons with small wave numbers (i.e., long wavelengths) and frequencies near the ferromagnetic resonance can be excited [7,8]. The second one is parametric pumping where the spin waves are excited at half of the frequency of the microwave magnetic field [8–10]. In this case, there is no upper limit for the wave numbers of these spin waves, and exchange magnons with short wavelengths can be excited. To our best knowledge, in all previous experiments (e.g., [3–5,11–13]) the spin pumping mechanism and the ISHE has been investigated only for the uniform precession or dipolar spin waves with long wavelengths.

In this Letter, we present the spin pumping effect by exchange magnons and its detection via the ISHE voltage in a ferrite-platinum bilayer structure. The magnons were injected in a ferrite film using the parametric mechanism. By varying the value of the magnetizing field we were able to change the wavelength of the magnons down to submicron values.

The sample used in the present study comprises a 2.1 $\mu$m thick single-crystal ferrite yttrium iron garnet (YIG, $Y_3Fe_5O_{12}$) film grown on a gallium gadolinium garnet (GGG) substrate by liquid phase epitaxy [see Fig. 1(a)]. A 10 nm thick $3 \times 3$ mm$^2$ platinum (Pt) layer is deposited onto the YIG film. The Pt pad is wired to a voltage preamplifier and an oscilloscope in order to detect the electromotive force $V_{\mathrm{ISHE}}$ generated by the ISHE. The magnetizing field $\vec{H}$ is applied in the standard orientation to observe the ISHE [4,5,11] so that the electron carried spin current (which propagates into the Pt layer from the YIG-Pt interface) and the ISHE-induced charge current are perpendicular to each other and to the field $\vec{H}$. Magnons

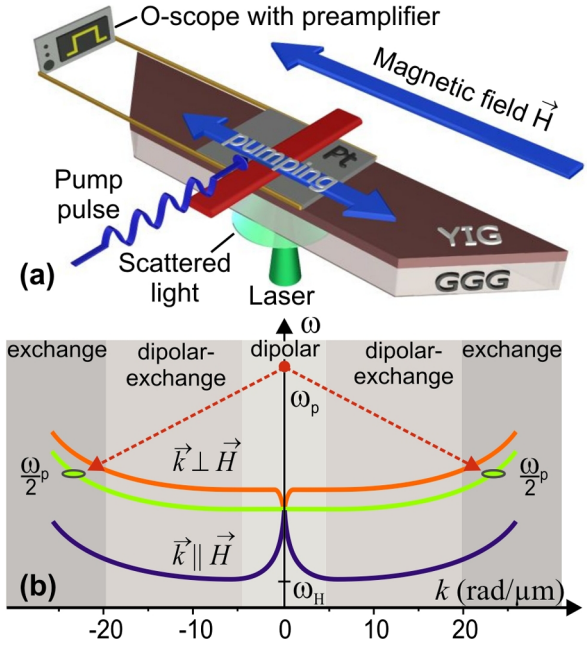


FIG. 1 (color online). (a) Sketch of the experimental setup. (b) The magnon spectrum and the mechanism of the parametric pumping process: One quantum of the pump field of $\omega_p$ frequency splits into two magnons of $\omega_p/2$ frequency.

 

contributing to the ISHE voltage are parametrically injected by a microwave Oersted field induced with a 50 $\mu$m-wide microstrip, which is insulated from the Pt layer by a thin nonmagnetic dielectric coating of cyanacrylate. Both parallel and perpendicular (relative to $\vec{H}$) components of the Oersted field contribute to the parametric pumping as has been shown in Ref. [14]. The pump frequency was held constant at 14 GHz, and the pump power $P$ was varied between 1.7 and 28.2 W. In order to reduce the microwave heat we used 5 $\mu$s-long microwave pulses with 50 $\mu$s repetition time rather than continuous waves. The magnons were detected by using Brillouin light scattering (BLS) spectroscopy: The probing light beam was focused on the YIG-Pt sample, and the inelastically scattered light, whose intensity is proportional to the quantity of magnons, was analyzed [15].

Figure 1(b) schematically illustrates the magnon spectrum (frequency $\omega$ vs wave number $k$) in a YIG film and the mechanism of parametric electromagnetic pumping. The entire spectrum, which comprises all possible directions of magnon propagation, can be separated in three different regions. In the area where magnons have small wave numbers, the dipolar interaction is dominant. In a region of $k$ from 1 to 20 rad/$\mu$m, the dispersion relations are influenced by both dipolar and exchange interactions. In the third area (above 20 rad/$\mu$m), only exchange magnons exist.

The electromagnetic pumping can be described in terms of energy quanta, where a single microwave photon (associating with the parallel component of the microwave Oersted field) or magnon (nonresonantly excited by the perpendicular component of the microwave field) with the frequency $\omega_p$ and near zero wave number splits into two magnons with $\omega_p/2$ but opposite wave vectors $\vec{k}$ and $-\vec{k}$. Because of the degeneracy in $\omega$, $k$ space, different magnon groups with the same frequency $\omega_p/2$ are pumped at the same time, but only one survives [9,10]. This group, the dominant group, is characterized by the lowest damping and the highest coupling to the pump field [9,10,14]. The dispersion curve corresponding to the dominant group is shown by the middle green line in Fig. 1(b). The variation of the magnetizing field $H$ at constant pump frequency results in a shifting of the whole spectrum up or down and in the tuning of the excited magnons wave numbers (see right panels in Fig. 2). The field $H$ was varied in the range from $-3000$ to 3000 Oe, allowing the excitation of both dipolar and exchange magnons.

The $V_{\mathrm{ISHE}}$ signal measured for $P = 8.9$ W at $H = 2750$ Oe is presented in Fig. 2(a). On the right-hand side, the sketch of the corresponding pumping process demonstrates that $\omega_p/2$ lies below the spin-wave spectrum and no parametric excitation can take place. In spite of this fact, a $V_{\mathrm{ISHE}}$ signal is detectable. This voltage $V_{\mathrm{SB}}$ is associated with the longitudinal spin-Seebeck effect [16]. It is independent of the value of the bias magnetic field $H$ and

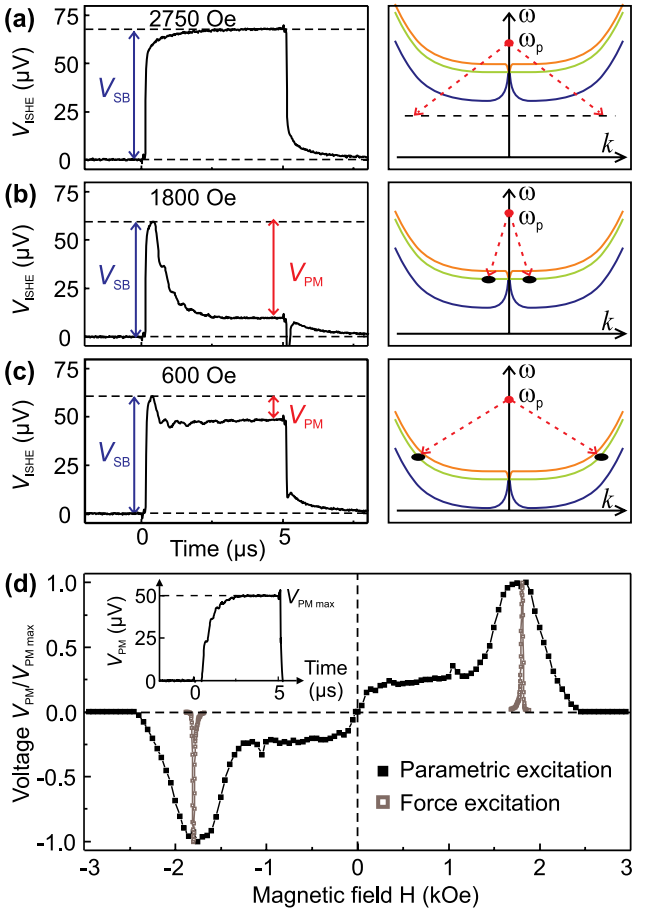


FIG. 2 (color online). (a)–(c) Waveforms of the $V_{\mathrm{ISHE}}$ voltage (left column) and pumping schemes for different magnetizing fields $H$. (d) Spin pumping induced voltage dependencies $V_{\mathrm{PM}}(H)$ for parametrically injected magnons (black filled squares) and force excited magnons (gray empty squares). The inset shows the time profile of the pure $V_{\mathrm{PM}}$ signal without spin-Seebeck effect contribution $V_{\mathrm{SB}}$ at $H = 1800$ Oe.

changes its polarity at $H = 0$. A temperature gradient $\nabla T$ perpendicular to the YIG surface (and parallel to the spin current) is created due to the heating of the Pt layer by eddy currents induced by the microwave pump field. The longitudinal spin-Seebeck effect can be explained with an imbalance between an effective magnon temperature in YIG and an effective conduction-electron temperature in the attached Pt layer [16,17]. The significant higher conduction-electron temperature in the Pt layer leads to thermal fluctuations and an ejection of spins to the YIG.

At $H = 1800$ Oe, as shown in Fig. 2(b), the situation is different since the $\omega_p/2$ frequency lies above the bottom of the magnon spectrum $\omega_H$ [see Fig. 1(b)], and excitation of the dipolar magnons is allowed. The time profile of the $V_{\mathrm{ISHE}}$ shows two opposing contributions. The first contribution $V_{\mathrm{SB}}$ belongs to the longitudinal spin-Seebeck effect, as in the former case. However, the second contribution $V_{\mathrm{PM}}$ can be attributed to the spin pumping by

parametrically excited magnons. In this process, spins are injected into the Pt layer, while in the longitudinal spin-Seebeck effect, spins are ejected from the Pt layer to the YIG. Thus, these two effects show different polarities in the voltage $V_{\mathrm{ISHE}}$. In addition, the voltage $V_{\mathrm{PM}}$ of the parametrically excited magnons is temporarily retarded since the equilibrium has to be established in the magnon system after the pump pulse is switched on. By subtracting the two contributions to the $V_{\mathrm{ISHE}}$ signal, the pure $V_{\mathrm{PM}}$ signal can be extracted [see the inset in Fig. 2(d)].

Figure 2(c) shows the situation for $H = 600$ Oe, where only magnons in the exchange area are injected. The $V_{\mathrm{ISHE}}$ profile shows again the two contributions to the electromotive force. The voltage $V_{\mathrm{PM}}$ due to the spin pumping by exchange magnons is clearly observable.

The extracted normalized voltage $V_{\mathrm{PM}}$ is presented in Fig. 2(d) for magnetic fields from $-3000$ to 3000 Oe. As expected, the curve is antisymmetrical with respect to the field polarity. For small values of $H$, the voltage goes to zero due to the sample demagnetization and formation of domains. For large fields ($|H| > 2400$ Oe), the voltage is zero as $\omega_p/2$ lies below the magnon spectrum and no parametric excitation can take place. The voltage maxima are visible around $H_c = \pm 1780$ Oe, where the minima of the parametric generation threshold are observed and the magnon injection is most effective.

The field $H_c$ usually corresponds to the situation when the $\omega_p/2$ frequency is in the vicinity of the ferromagnetic resonance frequency of the YIG film. In order to prove this, an additional experiment has been performed: Long-wavelength dipolar spin waves were excited by using the same microstrip by the microwave signal of $\omega_s = \omega_p/2 = 7$ GHz frequency and ISHE voltage was measured [see the narrow peaks in Fig. 2(d)]. The maxima of both dependencies coincide well.

The relatively small voltages $V_{\mathrm{PM}}$ in the exchange region ($|H| < 1300$ Oe) in comparison to the dipolar region ($1300 < |H| < 2400$ Oe) can be understood by analyzing the spatial localization of the dominant group taking into account the interface nature of the spin pumping effect [2,5,11]. This group is characterized by the smallest magnon damping, which is mostly determined by two-magnon scattering on inhomogeneities and impurities of the sample [9,18]. In single-crystal YIG films, these impurities are mainly localized close to the film surfaces. Thus, we may conclude that the dominant group is located in the middle of the YIG film where the scattering is the smallest. The localization of these magnons depends on their wavelengths, and it determines the intensity of the magnetization precession at the YIG-Pt interface. The shorter the wavelength, the higher the localization, and consequently the spin pumping is smaller due to the decreasing of the magnetization precession on the interface.

The calculated wavelength dependence of the excited magnons as a function of the applied bias magnetic field [see Eq. (7.9) in [9]] is shown in Fig. 3(a). One can see that the curve follows the voltage dependence shown in Figs. 2(d) and 3(b) qualitatively: In the exchange region, the wavelength as well as the ISHE-induced voltage does not change much. However, the increase of the field in the region 1300 Oe $< H < H_c$ results in a fast increase of the magnon wavelength as well as the detected voltage. Thus, the magnon wavelength and localization are of crucial importance for the spin pumping efficiency.

Note that a slight regular increase of the parametric generation threshold ($\simeq 4$ dB from $H_c$ to 250 Oe [14]) can also partially contribute to the observed voltage decrease in the exchange region [Fig. 3(b)]. However, for $H > H_c$ the threshold increases rapidly up to infinity at $\omega_p/2 = \omega_H$ [9,14]. This effect defines the voltage fall in the high field region.

The normalized field dependence of the ISHE-induced voltage for three different pump powers is shown in Fig. 3(b). One can see that the increase of the pump power and consequently the density of the parametrically injected magnons do not change qualitatively the voltage behavior. The small increase of the voltage slope in the exchange region can be associated with a nonlinear damping caused

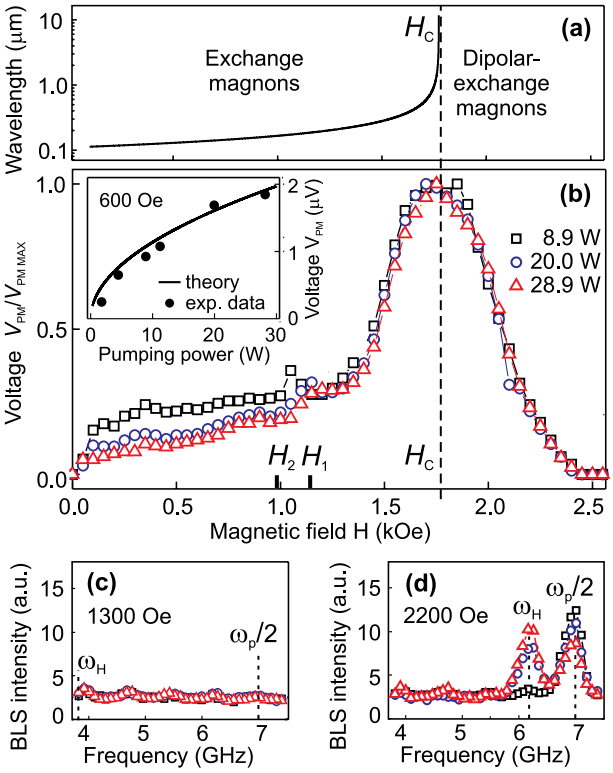


FIG. 3 (color online). (a) Calculated wavelength of the parametrically injected magnons. (b) Normalized dependencies $V_{\mathrm{PM}}(H)$ for different pump powers. The corresponding BLS spectra for two magnetic fields are shown in (c) and (d). The inset in (b) shows the ISHE signal of the parametrically excited magnons at 600 Oe for different pumping powers in comparison to the calculated power dependence.

by three-magnon scattering processes which for the given experimental conditions are allowed for fields smaller than the critical field $H_1 = 1150$ Oe [10,19].

Small peaks in the ISHE voltage, which are clearly visible in Fig. 2(d), appear just below the field $H_1$. They can be associated with the confluence of two parametrically injected magnons. Such a process occurs in the vicinity of the second critical field $H_2$ [10,19] (970 Oe for our experimental conditions). The angular momentum of one of the confluencing magnons is not conserved and must be passed to the entire sample lattice. This angular momentum may be directly passed to a free electron in the Pt layer. As a result the spin polarization of the electron gas will increase leading to the increase of the ISHE voltage.

The dependence of the ISHE voltage as a function of the pump power for the exchange region ($H = 600$ Oe) is shown in the inset in Fig. 3(b). The magnon density of the dominant group in the saturation regime is given by $n = \sqrt{(h_p V_k)^2 - \Gamma_k^2}/S$, where $S$ is a coefficient of the four-magnon scattering, $V_k$ describes the parametric coupling of a magnon group and the pump field, and $\Gamma_k$ is the magnon damping [10]. As $V_{\mathrm{PM}}$ is proportional to the magnon density, the experimental pump power $P_p$ is proportional to $(h_p V_k)^2$, and the threshold of parametric generation $P_{p\,\mathrm{thr}}$ (which is known from the experiment to be 25 mW) is proportional to $\Gamma_k^2$, we may rewrite this equation as $V_{\mathrm{PM}} \propto \sqrt{P_p - P_{p\,\mathrm{thr}}}$. The theoretical dependence $V_{\mathrm{PM}}(P_p)$ is in excellent agreement with the experiment.

The parametric pumping process results not only in the increase of the density of the dominant magnon group. Because of the four-magnon scattering, the redistribution of magnons over the whole magnon spectrum occurs. When the magnon density is sufficiently high, the condensation of magnons to the lowest energy state $\omega_H$ in the dipolar-exchange spectral area can occur [20]. In order to check that this process does not influence our results, an additional BLS characterization of the magnon gas was performed for different pump powers. The obtained data are presented in Fig. 3. In the case when the magnons are injected near the bottom of the magnon spectrum ($H = 2200$ Oe), one sees the pump power dependent redistribution of the injected magnons to the lowest energy states [Fig. 3(d)]. As is visible from Fig. 3(b), this redistribution practically does not influence the ISHE voltage. This is due to both the conservation of the total number of magnons in the four-magnon scattering process and the conservation of the magnon localization (the process develops in the dipolar-exchange region exclusively). For the small magnetizing field $H = 1300$ Oe when the exchange magnons are injected, no magnon redistribution is detected. (Note that the signal at $\omega_p/2$ is not observable as the wave number of the injected magnons 30 rad/$\mu$m overcomes the wave number limitation of the BLS setup.) This result shows that the only contribution to the spin pumping process comes from exchange magnons.

In conclusion, we demonstrate that exchange magnons of submicron wavelengths with no associated dipolar field significantly contribute to the spin pumping in magnetic and nonmagnetic bilayers. The spin pumping efficiency is mainly defined by localization of the injected magnons relative to the interlayer interface. The results are useful for the understanding of the physics of the spin pumping phenomenon and are of crucial importance for further miniaturization of the magnon-based spintronic devices as only short-wavelength exchange magnons allow signal processing on the nanoscale distance. Furthermore, the combination of the spin pumping and ISHE effects is the effective instrument for magnon detection beyond the wave number limitation of most existing methods including Brillouin light scattering spectroscopy.

Financial support by the DFG within the SFB/TRR 49, a Grant-in-Aid MEXT/JSPS, a Grant for Industrial Technology Research from NEDO, and Fundamental Research Grant from TRF, Japan is acknowledged.

*sandweg@physik.uni-kl.de

[1] S. A. Wolf *et al.*, Science **294**, 1488 (2001).
[2] Y. Tserkovnyak, A. Brataas, and G. E. W. Bauer, Phys. Rev. Lett. **88**, 117601 (2002).
[3] S. Mizukami, Y. Ando, and T. Miyazaki, Phys. Rev. B **66**, 104413 (2002).
[4] E. Saitoh *et al.*, Appl. Phys. Lett. **88**, 182509 (2006).
[5] Y. Kajiwara *et al.*, Nature (London) **464**, 262 (2010).
[6] K. Uchida *et al.*, Nature Mater. **9**, 894 (2010).
[7] A. K. Ganguly and D. C. Webb, IEEE Trans. Microwave Theory Tech. **23**, 998 (1975).
[8] A. A. Serga, A. V. Chumak, and B. Hillebrands, J. Phys. D **43**, 264002 (2010).
[9] A. G. Gurevich and G. A. Melkov, *Magnetization Oscillations and Waves* (CRC, New York, 1996).
[10] V. S. L'vov, *Wave Turbulence under Parametric Excitations: Applications to Magnetics* (Springer, Berlin, 1994).
[11] C. W. Sandweg *et al.*, Appl. Phys. Lett. **97**, 252504 (2010).
[12] K. Ando *et al.*, Appl. Phys. Lett. **94**, 262505 (2009).
[13] M. V. Costache *et al.*, Phys. Rev. Lett. **97**, 216603 (2006).
[14] T. Neumann *et al.*, Appl. Phys. Lett. **94**, 192502 (2009).
[15] S. O. Demokritov, B. Hillebrands, and A. N. Slavin, Phys. Rep. **348**, 441 (2001).
[16] K. Uchida *et al.*, Appl. Phys. Lett. **97**, 172505 (2010).
[17] J. Xiao *et al.*, Phys. Rev. B **81**, 214418 (2010).
[18] M. Sparks, *Ferromagnetic Relaxation Theory* (McGraw-Hill, New York, 1964).
[19] V. S. L'vov and G. E. Fal'kovich, Sov. Phys. JETP **55**, 904 (1982).
[20] S. O. Demokritov *et al.*, Nature (London) **443**, 430 (2006).